

## Chapter 3

### Lecture 7

#### Drag polar – 2

#### Topics

- 3.2.3 Summary of lift coefficient, drag coefficient, pitching moment coefficient, centre of pressure and aerodynamic centre of an airfoil
- 3.2.4 Examples of pressure coefficient distributions
- 3.2.5 Introduction to boundary layer theory
- 3.2.6 Boundary layer over a flat plate – height of boundary layer, displacement thickness and skin friction drag

#### **3.2.3 Summary of the lift coefficient, drag coefficient, pressure coefficient, pitching moment coefficient, centre of pressure and aerodynamic centre of an airfoil**

In order to understand the dependence of pressure drag and skin friction drag on various factors, it is appropriate, at this stage, to present brief discussions on (I) generation of lift, drag and pitching moment from the distributions of pressure ( $p$ ) and shear stress ( $\tau$ ) and (II) outline of boundary layer theory. These and the related topics are covered in this subsection and in the subsections 3.2.4 to 3.2.10. In subsections 3.2.11 to 3.2.13 the airfoil characteristics and their nomenclature are dealt with. Subsequently, the estimation of the drags of wing, fuselage and the entire airplane at subsonic speeds are discussed (sections 3.2.14 to 3.2.21).

Figure 3.7 shows an airfoil at an angle of attack ( $\alpha$ ) kept in a stream of velocity  $V_\infty$ . The resultant aerodynamic force ( $R$ ) is produced due to the distributions of the shear stress ( $\tau$ ) and the pressure ( $p$ ). The distributions also produce a pitching moment ( $M$ ). By definition, the component of  $R$  perpendicular to the free stream direction is called lift ( $L$ ) and the component along the free stream direction is called drag ( $D$ ). The resultant aerodynamic force ( $R$ ) can also

Flight dynamics-I  
Chapter-3

be resolved along and perpendicular to the chord of the airfoil. These components can be denoted by C and N respectively(Fig.3.7). From the subsequent discussion in this section, it will be evident that it is more convenient to evaluate N and C from the distributions of shear stress ( $\tau$ ) and pressure ( $p$ ) and then evaluate L and D.

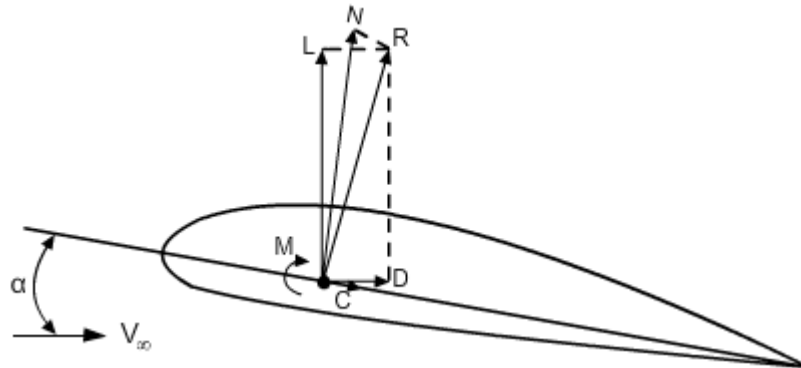


Fig.3.7 Aerodynamic forces and moment on an airfoil

From Fig.3.7 it can be deduced that :

$$L = N \cos \alpha - C \sin \alpha \quad (3.7)$$

$$D = N \sin \alpha + C \cos \alpha \quad (3.8)$$

Figure 3.8 shows elements of length and  $ds_u$  and  $ds_l$  at points  $P_u$  and  $P_l$  on the upper and lower surfaces of the airfoil respectively. The cartesian coordinates of points  $P_u$  and  $P_l$  are  $(x_u, y_u)$  and  $(x_l, y_l)$  respectively. Whereas  $s_u$  and  $s_l$  are respectively the distances along the airfoil surface, of the points  $P_u$  and  $P_l$  measured from the stagnation point (Fig.3.8).

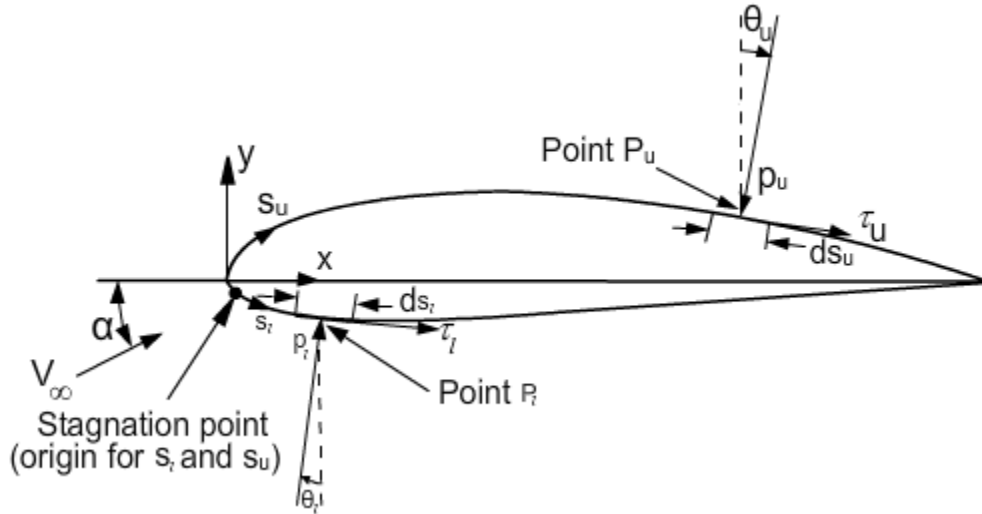


Fig.3.8 Pressure and shear stress at typical points on upper and lower surfaces of an airfoil

To obtain the forces at points  $P_u$  and  $P_l$ , the local values of  $p$  and  $\tau$  are multiplied by the local area. Since the flow past an airfoil is treated as two-dimensional, the span of the airfoil can be taken as unity without loss of generality. Hence, the local area is  $(ds \times 1)$  and the quantities,  $L$ ,  $D$ ,  $N$  and  $C$ , on the airfoil, are the forces per unit span. Keeping these in mind, the local contributions,  $dN_u$  and  $dC_u$ , to  $N$  and  $C$  respectively, from the element at point  $P_u$  are obtained as:

$$dN_u = -p_u ds_u \cos \theta_u - \tau_u ds_u \sin \theta_u \quad (3.9)$$

$$dC_u = -p_u ds_u \sin \theta_u + \tau_u ds_u \cos \theta_u \quad (3.10)$$

Note that the suffix 'u' denotes quantities at point  $P_u$  and the positive direction of the angle  $\theta_u$  is as shown in Fig.3.8 .

Expressions similar to Eqs.(3.9) and (3.10) can be written down for the contributions to  $N$  and  $C$  from element at point  $P_l$ .

Integrating over the entire airfoil yields :

$$N = - \oint_{\text{upper surface}} (p_u \cos \theta_u + \tau_u \sin \theta_u) ds_u + \oint_{\text{lower surface}} (p_l \cos \theta_l - \tau_l \sin \theta_l) ds_l \quad (3.11)$$

$$C = \oint_{\text{upper surface}} (-p_u \sin \theta_u + \tau_u \cos \theta_u) ds_u + \oint_{\text{lower surface}} (p_l \sin \theta_l + \tau_l \cos \theta_l) ds_l \quad (3.12)$$

Proceeding in a similar manner, it can be shown that  $M_{le}$ , the pitching moment about leading edge of the airfoil, per unit span, is :

$$M_{le} = \oint_{\text{upper surface}} [(p_u \cos \theta_u + \tau_u \sin \theta_u) x_u - (p_u \sin \theta_u - \tau_u \cos \theta_u) y_u] ds_u + \oint_{\text{lower surface}} [(-p_l \cos \theta_l + \tau_l \sin \theta_l) x_l + (p_l \sin \theta_l + \tau_l \cos \theta_l) y_l] ds_l \quad (3.13)$$

**Note:** Once N and C are known, the lift per unit span (L) and drag per unit span (D) of the airfoil can be obtained using Eqs.(3.7) and (3.8).

It is convenient to work in terms of lift coefficient ( $C_l$ ) and drag coefficient ( $C_d$ ). The definitions of these may be recalled as :

$$C_l = \frac{L}{\frac{1}{2} \rho V_\infty^2 c} \quad (3.14)$$

and 
$$C_d = \frac{D}{\frac{1}{2} \rho V_\infty^2 c} \quad (3.15)$$

It may be pointed out, that integration of a constant pressure, say  $p_\infty$ , around the body would not give any resultant force i.e.

$$\oint p_\infty ds = 0 \quad (3.16)$$

Hence, instead of 'p' the quantity  $(p - p_\infty)$  can be used in Eqs.(3.11), (3.12) and (3.13). At this stage the following quantities are also defined.

pressure coefficient : 
$$C_p = \frac{p - p_\infty}{\frac{1}{2} \rho V_\infty^2} \quad (3.17)$$

skin friction drag coefficient : 
$$c_f = \frac{\tau}{\frac{1}{2} \rho V_\infty^2} \quad (3.18)$$

Flight dynamics-I  
Chapter-3

$$\left. \begin{aligned}
 \text{Normal force coefficient:} \quad C_n &= \frac{N}{\frac{1}{2}\rho V_\infty^2 c} \\
 \text{Chordwise or axial force coefficient:} \quad C_c &= \frac{C}{\frac{1}{2}\rho V_\infty^2 c} \\
 \text{Pitching moment coefficient:} \quad C_{mle} &= \frac{M_{le}}{\frac{1}{2}\rho V_\infty^2 c^2}
 \end{aligned} \right\} \quad (3.19)$$

It may be noted that  $dx = ds \cos \theta$  and  $dy = -ds \sin \theta$ , where “ $ds$ ” is an elemental length around a point P on the surface and  $\theta$  is the angle between the normal to the element and the vertical (Fig.3.8). Note that  $\theta$  is measured positive in the clockwise sense. It can be shown that :

$$\left. \begin{aligned}
 C_n &= \frac{1}{c} \left[ \int_0^c (C_{pl} - C_{pu}) dx + \oint_{\text{upper surface}} c_{fu} dy + \oint_{\text{lower surface}} c_{fl} dy \right] \\
 C_c &= \frac{1}{c} \left[ \int_0^c (c_{fu} + c_{fl}) dx + \oint_{\text{upper surface}} C_{pu} dy - \oint_{\text{lower surface}} C_{pl} dy \right]
 \end{aligned} \right\} \quad (3.20)$$

Following section 10.2 of Ref.1.4, the expressions for  $C_n$ ,  $C_c$  and  $C_{mle}$  can be rewritten as:

$$\left. \begin{aligned}
 C_n &= \frac{1}{c} \left[ \int_0^c (C_{pl} - C_{pu}) dx + \int_0^c \left( c_{fu} \frac{dy_u}{dx} + c_{fl} \frac{dy_l}{dx} \right) dx \right] \\
 C_c &= \frac{1}{c} \left[ \int_0^c \left( C_{pu} \frac{dy_u}{dx} - C_{pl} \frac{dy_l}{dx} \right) dx + \int_0^c (c_{fu} - c_{fl}) dx \right] \\
 C_{mle} &= \frac{1}{c^2} \left[ \int_0^c (C_{pu} - C_{pl}) x dx - \int_0^c \left( C_{fu} \frac{dy_u}{dx} + c_{fl} \frac{dy_l}{dx} \right) x dx \right] \\
 &\quad + \frac{1}{c^2} \left[ \int_0^c \left( C_{pu} \frac{dy_u}{dx} + c_{fu} \right) y_u dx + \int_0^c \left( -C_{pl} \frac{dy_l}{dx} + c_{fl} \right) y_l dx \right]
 \end{aligned} \right\} \quad (3.21)$$

**Remarks:**

(i) From  $C_n$  and  $C_c$  the lift coefficient ( $C_l$ ) and drag coefficient ( $C_d$ ) are obtained as :

$$C_l = C_n \cos \alpha - C_c \sin \alpha \quad (3.22)$$

$$C_d = C_n \sin \alpha + C_c \cos \alpha \quad (3.23)$$

(ii) **Centre of pressure** : The point on the airfoil chord through which the resultant aerodynamic force passes is the centre of pressure. The aerodynamic moment about this point is zero. It may be noted that the location of centre of pressure depends on the angle of attack or the lift coefficient.

(iii) **Aerodynamic centre**: As the location of the centre of pressure depends on lift coefficient ( $C_l$ ) the pitching moment coefficient about leading edge ( $C_{mle}$ ) also changes with  $C_l$ . However, it is found that there is a point on the airfoil chord about which the pitching moment coefficient is independent of the lift coefficient. This point is called 'Aerodynamic centre'. For incompressible flow this point is close to the quarter chord point of the airfoil.

(iv) If the distributions of  $C_p$  and  $c_f$  are obtained by analytical or computational methods, then the pressure drag coefficient ( $C_{dp}$ ) and the skin friction drag coefficient ( $C_{df}$ ) can be evaluated.

In experimental work the pressure distribution on an airfoil at different angles of attack can be easily measured. However, measurement of shear stress ( $\tau$ ) on an airfoil surface is difficult. The profile drag coefficient ( $C_d$ ) of airfoil, which is the sum of pressure drag coefficient and skin friction drag coefficient, is measured in experiments by 'Wake survey technique' which is described in Chapter 9, section 'f' of Ref.3.10. In this technique, the momentum loss due to the presence of the airfoil is calculated and equated to the drag (refer section 7.5.1 of Ref.3.11 for derivation).

### 3.2.4 Examples of pressure coefficient distributions

Though the expression for lift coefficient ( $C_l$ ) involves both the pressure coefficient ( $C_p$ ) and the skin friction drag coefficient ( $c_f$ ), the contribution of the

Flight dynamics-I  
Chapter-3

former i.e.  $C_p$  is predominant to decide  $C_l$ . On the other hand, the pressure drag coefficient ( $C_{dp}$ ) is determined by the distribution of  $C_p$  and the skin friction drag coefficient ( $C_{df}$ ) is decided by the distribution of shear stress ( $\tau$ ).

In this subsection the distributions of  $C_p$  in typical cases and their implications for  $C_l$  and  $C_{dp}$  are discussed.

The distribution of the pressure coefficient is generally plotted on the outer side of the surface of the body (Fig.3.9a). The length of the arrow indicates the magnitude of  $C_p$ . As regards the sign convention, an arrow pointing towards the surface indicates that  $C_p$  is positive or local pressure is more than the free stream pressure ( $p_\infty$ ). An arrow pointing away from the surface indicates that  $C_p$  is negative i.e. the local pressure is lower than ( $p_\infty$ ).

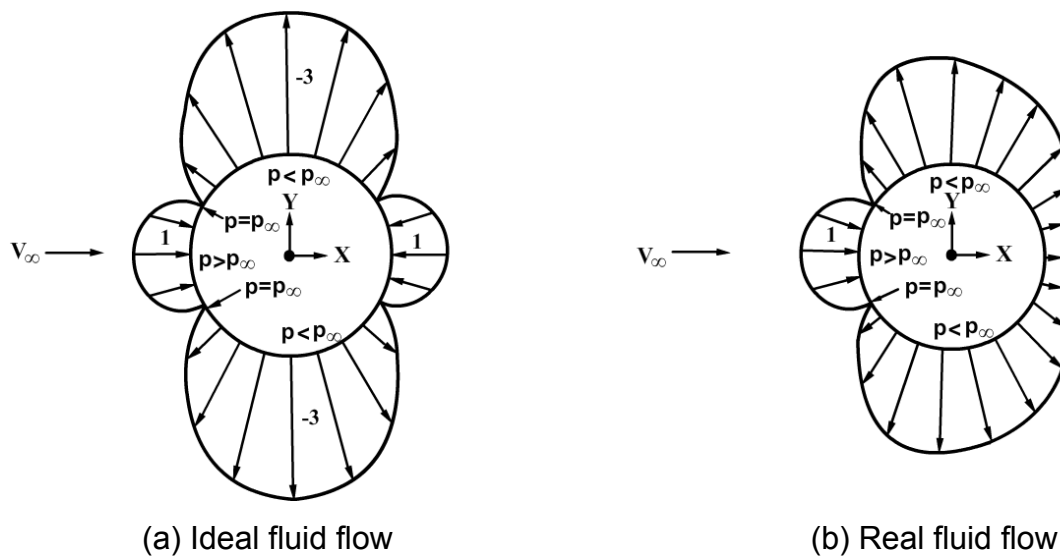


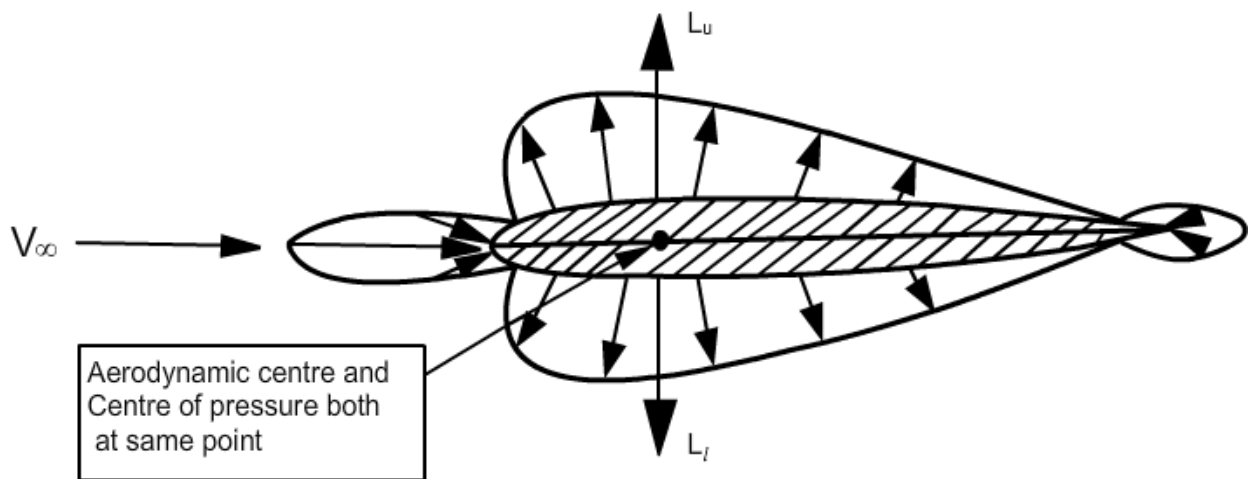
Fig.3.9 Distribution of  $C_p$  around a circular cylinder

Figure 3.9 shows distributions of  $C_p$  in ideal fluid flow and real fluid flow past a circular cylinder. It may be recalled that an ideal fluid is inviscid and incompressible whereas a real fluid is viscous and compressible. From the distribution of  $C_p$  in ideal fluid flow (Fig.3.9a) it is seen that the distribution is symmetric about X-axis and Y-axis. It is evident that in this case, the net forces in vertical and horizontal directions are zero. This results in  $C_l = 0$ ,  $C_{dp} = 0$ . These results are available in books on fluid mechanics and aerodynamics. In the real

Flight dynamics-I  
Chapter-3

fluid flow case, shown in Fig.3.9b, it is seen that the flow separates from the body (see description on boundary layer separation in section 3.2.7) and the pressure coefficient behind the cylinder is negative and nearly constant. However, the distribution is still symmetric about horizontal axis. Thus in this case  $C_l = 0$  but  $C_{dp} > 0$ .

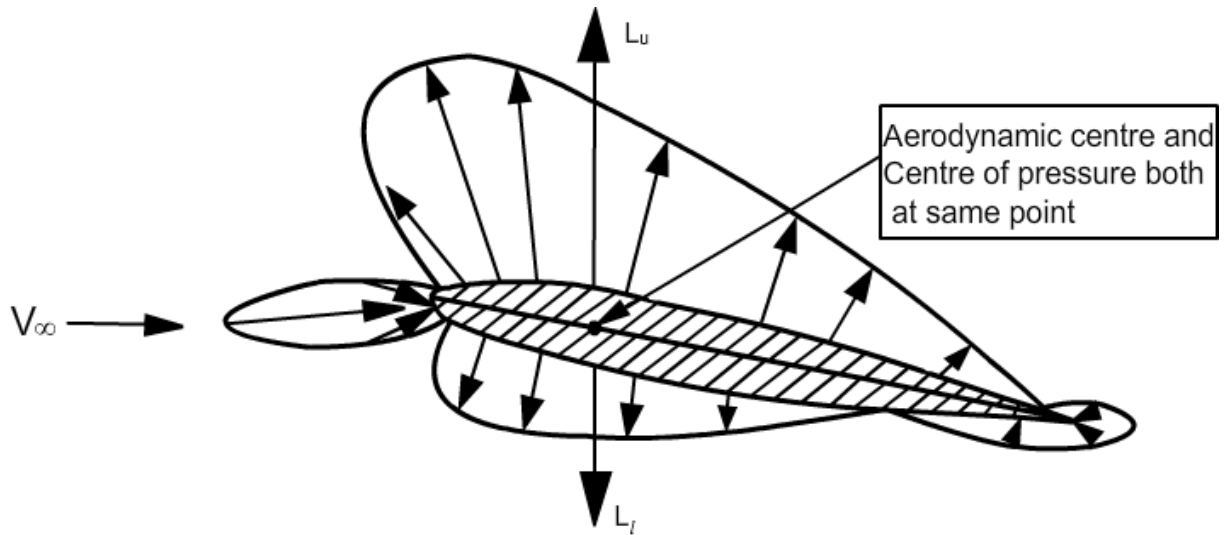
The distributions of  $C_p$  over symmetrical and unsymmetrical foils at  $C_l = 0$  and  $C_l > 0$  are shown in Figs.3.10 a to d. Note also the locations of centre pressure and the production of pitching moment for the unsymmetrical airfoil. Flow visualization pictures at three angles of attack ( $\alpha$ ) are shown in Figs.3.36 a, b and c. An attached flow is seen at low angle of attack. Some separated flow is seen at moderate angle of attack and large separated flow region is seen near  $\alpha$  close to the stalling angle ( $\alpha_{stall}$ ). It may be pointed out that theoretical calculation of skin friction drag using boundary layer theory can be done, when flow is attached. This topic is discussed in the next subsection.



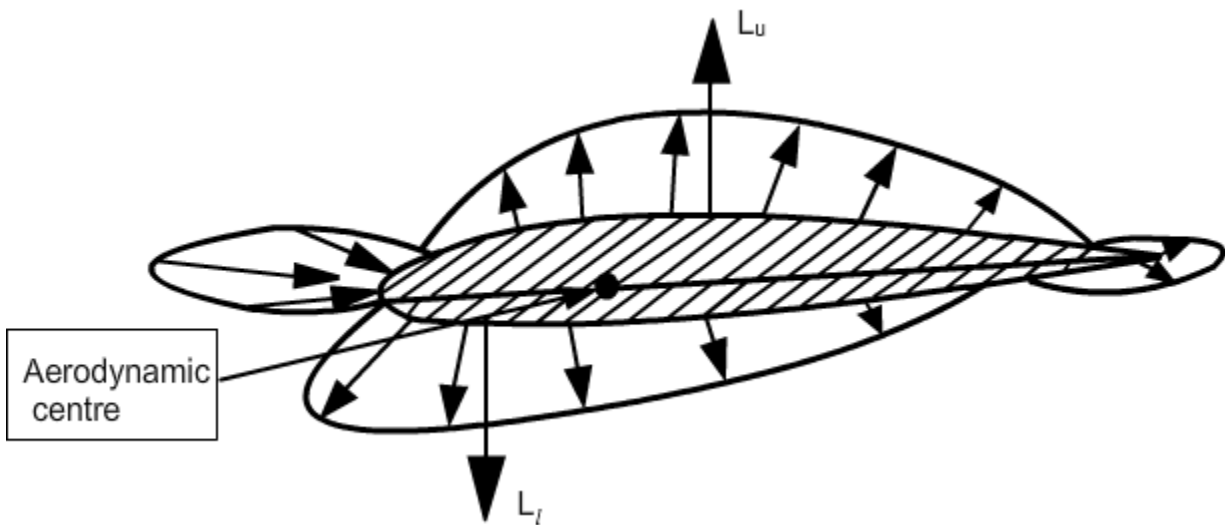
(a) Distribution of pressure coefficient on symmetrical airfoil at  $C_l = 0$  and  $\alpha = 0$

**Note :**  $L_u = L_l$



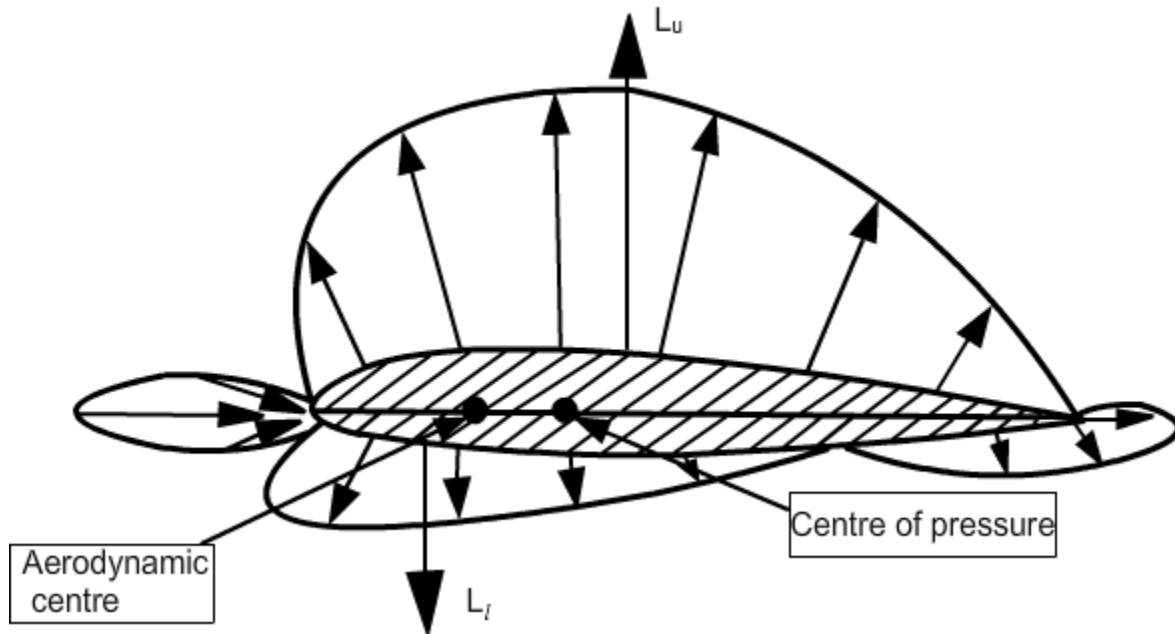


(b) Distribution of pressure coefficient on symmetrical airfoil at  $C_l > 0$  and  $\alpha > 0$



(c) Distribution of pressure coefficient on cambered airfoil at  $C_l = 0$ ,  $\alpha < 0$  ;

**Note:**  $L_u$  and  $L_l$  form a couple; centre of pressure is at infinity,  $C_{mac} < 0$ ,



(d) Distribution of pressure coefficient on cambered airfoil at  $C_l > 0$ ,  $\alpha > 0$

Note :  $C_{mac}$  same as in Fig.(c)

Fig.3.10 Distributions of pressure coefficient on symmetrical and unsymmetric airfoils at  $C_l = 0$  and  $C_l > 0$

### 3.2.5 Introduction to boundary layer theory

Under conditions of normal temperature and pressure a fluid satisfies the 'No slip condition' i.e. on the surface of a solid body the relative velocity between the fluid and the solid wall is zero. Thus, when the body is at rest the velocity of the fluid layer on the body is zero. In this and the subsequent subsections, the body is considered to be at rest and the fluid moving past it. Though the velocity is zero at the surface, a velocity of the order of free stream velocity is reached in a very thin layer called 'Boundary layer'. The velocity gradient normal to the

surface  $\left(\frac{\partial U}{\partial y}\right)$  is very high in the boundary layer. Hence even if the coefficient of

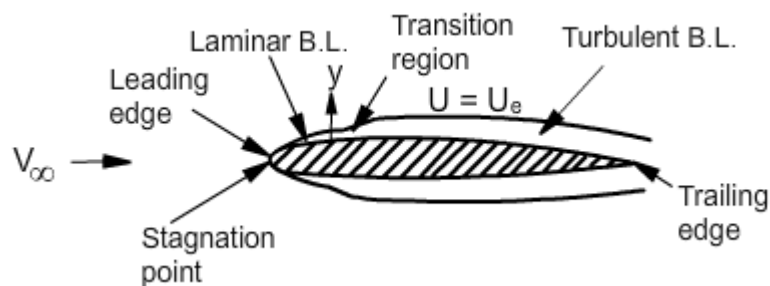
viscosity ( $\mu$ ) is small, the shear stress,  $\mu\left(\frac{\partial U}{\partial y}\right)$ , in the boundary layer may be

large or comparable to other stresses like pressure. Outside the boundary layer

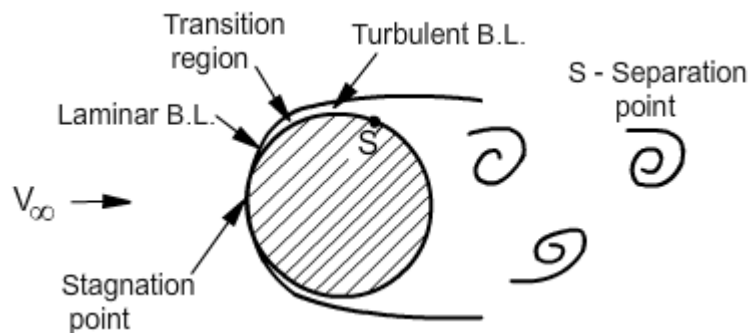
Flight dynamics-I  
Chapter-3

the gradient ( $\partial U / \partial y$ ) is very small and viscous stress can be ignored and flow treated as inviscid. It may be recalled from text books on fluid mechanics, that in an inviscid flow the Bernoulli's equation is valid.

Features of the boundary layer over the surface of a streamlined body are shown in Fig.3.11a. On the surface of a bluff body the boundary layer develops upto a certain extent and then separates (Fig.3.11b). The definitions of the streamlined body and bluff body are presented at the end of this subsection.



(a) boundary layer over a streamlined body



(b) Boundary layer over a bluff body

Fig.3.11 Boundary layer over different shapes (not to scale)

## Flight dynamics-I

### Chapter-3

The features of the flow are as follows.

1. Near the leading edge (or the nose) of the body the flow is brought to rest. This point is called the 'Stagnation point'. A laminar boundary layer develops on the surface starting from that point. It may be recalled, from topics on fluid mechanics, that in a steady laminar flow the fluid particles move downstream in smooth and regular trajectories; the streamlines are invariant and the fluid properties like velocity, pressure and temperature at a point remain the same with time. In an unsteady laminar flow the fluid properties at a point may vary but are known functions of time. In a turbulent flow, on the other hand, the fluid properties at a point are random functions of time. However, the motion is organized in such a way that statistical averages can be taken. In a laminar boundary layer the parameter which mainly influence its development is the Reynolds number ( $R_x = \rho U_e x / \mu$ );  $x$  being distance along the surface, from the stagnation point.

2. Depending on the Reynolds number ( $R_x$ ), the pressure gradient and other parameters, the boundary layer may separate or become turbulent after undergoing transition. The turbulent boundary layer may continue till the trailing edge of the body (Fig.3.11a) or may separate from the surface of the body (point 'S' in Fig 3.11b). It may be added that the static pressure across the boundary layer at a station 'x', is nearly constant with 'y'. Hence the pressure gradient referred here is the gradient ( $dp/dx$ ) in the flow outside the boundary layer.

3. Nature of boundary layer decides the drag and the heat transfer from the body. If the boundary layer is separated, the pressure in the rear portion of the body does not reach the freestream value resulting in a large pressure drag (Fig.3.9b). Incidentally a streamlined body is one in which the major portion of drag is skin friction drag. For a bluff body the major portion of drag is pressure drag. A circular cylinder is a bluff body. An airfoil at low angle of attack is a streamlined shape. But, an airfoil at high angle of attack like  $\alpha_{stall}$  is a bluff body.

#### **Remark:**

General discussion on boundary layer is a specialised topic and the interested reader may consult Ref.3.11 for more information. Here, the features

of the laminar and turbulent boundary layers on a flat plate are briefly described. While discussing separation, the boundary layer over a curved surface is considered.

### 3.2.6 Laminar boundary layer over flat plate – height of boundary layer, displacement thickness and skin friction drag

The equations of motion governing the flow of a viscous fluid are called 'Navier-Stokes (N-S) equations'. For derivation of these equations refer to chapter 15 of Ref.3.12. Taking into account the thinness of the boundary layer, Prandtl simplified the N-S equations in 1904. These equations are called 'Boundary layer equations' (Chapter 16 of Ref.3.12). Solution of these equations, for laminar boundary layer over a flat plate with uniform external stream, was obtained by Blasius in 1908. Subsequently many others obtained the solution. The numerical solution by Howarth, presented in Ref.3.10, chapter 7, is given in Table 3.2. In this table  $U$  is the local velocity,  $U_e$  is the external velocity (which in this particular case is  $V_\infty$ ), and  $\eta$  is the non-dimensional distance from the wall defined as :

$$\eta = y \sqrt{\frac{U_e}{\nu x}} \quad (3.24)$$

$\eta$	0	0.2	0.4	0.6	0.8	1.0	1.2	1.4
$U/U_e$	0	0.06641	0.13277	0.19894	0.26471	0.32979	0.39378	0.45627
$\eta$	1.6	1.8	2.0	2.2	2.4	2.6	2.8	3.0
$U/U_e$	0.51676	0.57477	0.62977	0.68132	0.72899	0.77246	0.81752	0.84605
$\eta$	3.2	3.4	3.6	3.8	4.0	4.2	4.4	4.6
$U/U_e$	0.87609	0.90177	0.92333	0.94112	0.95552	0.96696	0.97587	0.98269
$\eta$	4.8	5.0	5.2	5.6	6.0	7.0	7.8	
$U/U_e$	0.98779	0.99155	0.99425	0.99748	0.99898	0.99992	1.0000	

Table 3.2 Non-dimensional velocity profile in a laminar boundary layer over a flat plate

### Height of boundary layer

It is seen from table 3.2 that the external velocity ( $U_e$ ) is attained very gradually. Hence the height at which  $U/U_e$  equals 0.99 is taken as the height of the boundary layer and denoted by  $\delta_{0.99}$ . From table 3.2,  $U/U_e \approx 0.99$  is attained at  $\eta = 5$ . Noting the definition of  $\eta$  in Eq.(3.24) gives :

$$5 = \delta_{0.99} \sqrt{\frac{U_e}{\nu x}}$$

Or 
$$\frac{\delta_{0.99}}{x} = \frac{5}{\sqrt{\frac{U_e x}{\nu}}} = \frac{5}{\sqrt{R_x}}; R_x = \frac{U_e x}{\nu} \quad (3.25)$$

Flight dynamics-I  
Chapter-3

Figure 3.12 shows a typical non-dimensional velocity profile in a laminar boundary layer. While presenting such a profile, it is a common practice to plot  $U/U_e$  on the abscissa and  $(y/\delta_{0.99})$  on the ordinate.

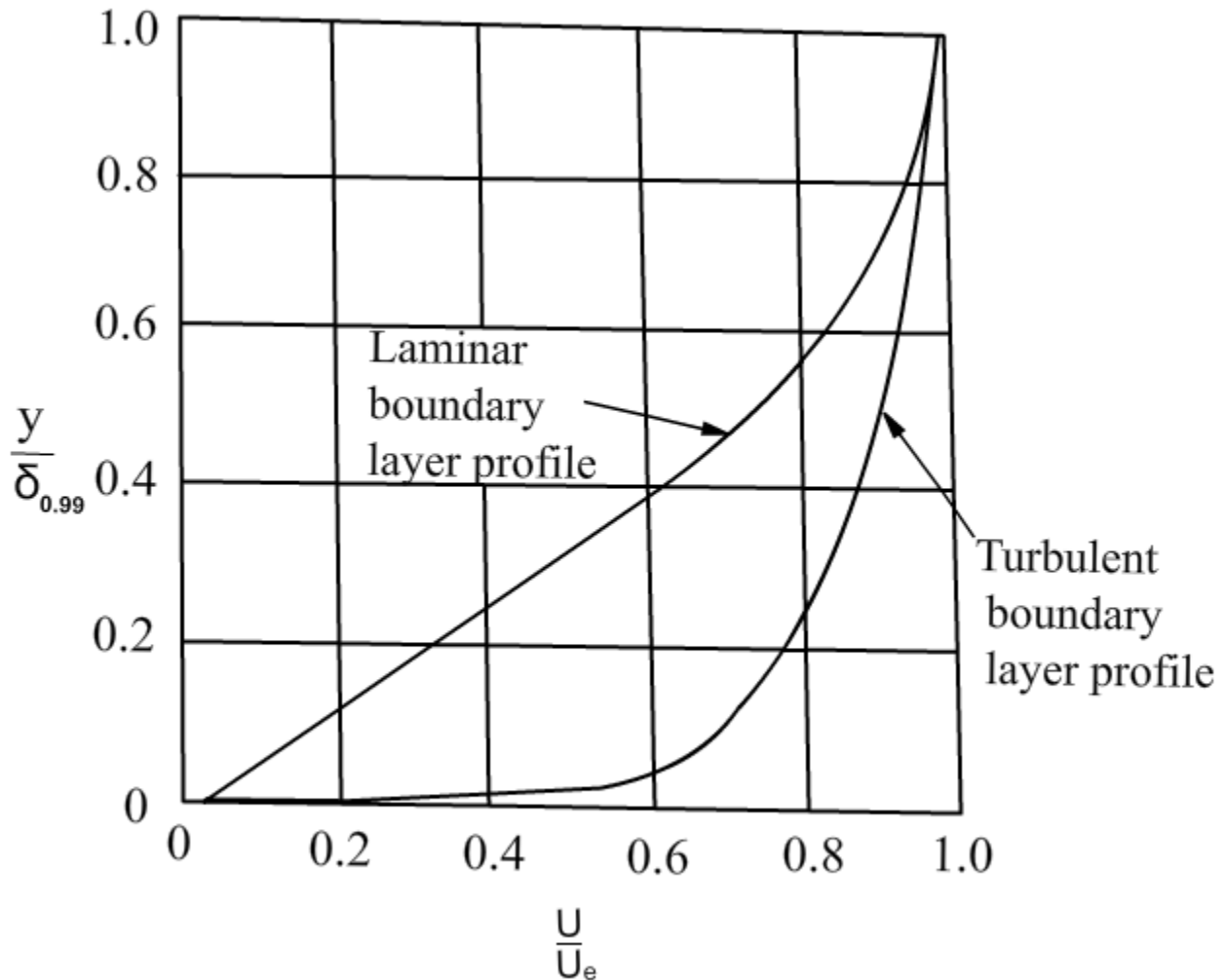


Fig.3.12 Non-dimensional velocity profile in laminar and turbulent boundary layers on a flat plate

It is seen from Eq.(3.25) that  $\delta_{0.99}$  grows in proportion to  $x^{\frac{1}{2}}$  (see Fig.3.13). It may be added that in this special case of laminar boundary layer on flat plate, the velocity profiles are similar at various stations i.e. the non-dimensional profiles of  $U/U_e$  vs  $(y/\delta_{0.99})$  are same at all stations.

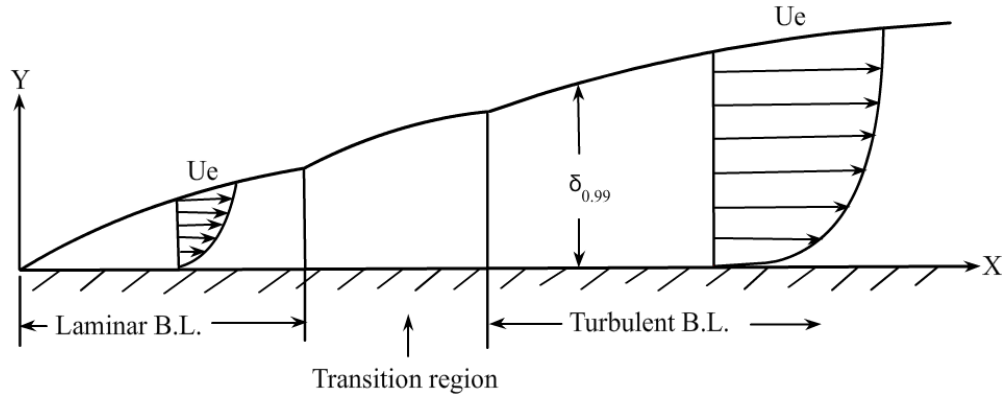


Fig.3.13 Schematic growth of boundary layer

### Displacement thickness and skin friction drag coefficient

The presence of boundary layer causes displacement of fluid and skin friction drag. The displacement thickness ( $\delta_1$ ) is defined as :

$$\delta_1 = \int_0^{\infty} \left(1 - \frac{U}{U_e}\right) dy \quad (3.26)$$

The local skin friction coefficient ( $C'_f$  or  $c_f$ ) is defined as :

$$C'_f = c_f = \frac{\tau_{wall}}{\frac{1}{2}\rho U_e^2}; \quad \tau_{wall} = \mu \left(\frac{\partial u}{\partial y}\right)_{y=0}; \quad \text{Note: } \tau_{wall} \text{ is a function of 'x'}. \quad (3.27)$$

If the length of the plate is L, then the skin friction drag per unit span of the plate ( $D_f$ ) is :

$$D_f = \int_0^L \tau_{wall} dx$$

Hence, skin friction drag coefficient  $C_{df}$  is given by:

$$C_{df} = \frac{D_f}{\frac{1}{2}\rho V_{\infty}^2 L} \quad (3.28)$$

From the boundary layer profile (table 3.2) it can be shown that for a flat plate of length, L, the expressions for  $\delta_1$  and  $C_{df}$  are:

$$\frac{\delta_1}{L} = \frac{1.721}{\sqrt{R_L}} \quad (3.29)$$



Flight dynamics-I  
Chapter-3

$$C_{df} = \frac{1.328}{\sqrt{R_L}}; R_L = \frac{V_\infty L}{\nu} \quad (3.30)$$

**Remark :**

Reference 1.11, chapter 6 may be consulted for additional boundary layer parameters like momentum thickness ( $\delta_2$ ), shape parameter ( $H = \delta_1/\delta_2$ ) and energy thickness ( $\delta_3$ ) of a boundary layer.

**Example 3.1**

Consider a flat plate of length 500 mm kept in an air stream of velocity 15 m/s. Obtain (a) the boundary layer thickness ( $\delta_{0.99}$ ) and the displacement thickness ( $\delta_1$ ) at the end of the plate (b) the skin drag coefficient. Assume  $\nu = 15 \times 10^{-6} \text{ m}^2/\text{s}$  and the boundary layer to be laminar.

**Solution:**

$$L = 0.5 \text{ m}, V_\infty = 15 \text{ m/s}, \nu = 15 \times 10^{-6} \text{ m}^2/\text{s}$$

$$\text{Hence, } R_L = \frac{0.5 \times 15}{15 \times 10^{-6}} = 5 \times 10^5$$

Consequently, from Eq.(3.25):

$$\frac{\delta_{0.99}}{L} = \frac{5}{\sqrt{R_L}} = \frac{5}{\sqrt{5 \times 10^5}} = 7.07 \times 10^{-3}$$

$$\text{Or } \delta_{0.99} = 7.07 \times 10^{-3} \times 0.5 = 3.54 \times 10^{-3} \text{ m} = 3.54 \text{ mm}$$

From Eq.(3.29):

$$\frac{\delta_1}{L} = \frac{1.721}{\sqrt{R_L}} = \frac{1.721}{\sqrt{5 \times 10^5}} = 2.434 \times 10^{-3}$$

$$\text{Or } \delta_1 = 2.434 \times 10^{-3} \times 0.5 = 1.217 \times 10^{-3} \text{ m} = 1.217 \text{ mm}$$

From Eq.(3.30):

$$C_{df} = \frac{1.328}{\sqrt{R_L}} = \frac{1.328}{\sqrt{5 \times 10^5}} = 0.00188$$

**Remark:**

( $\delta_{0.99}/L$ ) is found to be  $7.07 \times 10^{-3}$ . Hence the assumption of the thinness of boundary layer is confirmed by the results.